Current Opinion in Green and Sustainable Chemistry, 2022, Vol.33, art.100558. https://doi.org/10.1016/j.cogsc.2021.100558

Review article

Design of materials for solid oxide fuel cells, permselective membranes, and catalysts for biofuel transformation into syngas and hydrogen based on fundamental studies of their real structure, transport properties, and surface reactivity

Vladislav A. Sadykov [1,2], Nikita F. Eremeev [1], Ekaterina M. Sadovskaya [1,2], Anna V. Shlyakhtina [3], Elena Yu. Pikalova [4,5], Denis A. Osinkin [4,5], Aleksey A. Yaremchenko [6]

[1] *Federal Research Center Boreskov Institute of Catalysis SB RAS, av. Lavrentieva, 5, 630090, Novosibirsk, Russia*
[2] *Novosibirsk State University, 630090, Novosibirsk, Russia*
[3] *Federal Research Center Semenov Institute of Chemical Physics RAS, 119991, Moscow, Russia*
[4] *Institute of High-Temperature Electrochemistry UB RAS, 620137, Ekaterinburg, Russia*
[5] *Ural Federal University, 620002, Ekaterinburg, Russia*
[6] *CICECO – Aveiro Institute of Materials, Department of Materials and Ceramic Engineering, University of Aveiro, 3810-193, Aveiro, Portugal*

Corresponding author: Sadykov, Vladislav A. (sadykov@catalysis.ru)

Abstract

Advances in design of materials for solid oxide fuel cells, oxygen and hydrogen separation membranes, and catalysts for biofuel conversion into syngas and hydrogen are reviewed. Application of new efficient techniques of material synthesis and characterization of their atomic-scale structure, transport properties, and reactivity allowed to develop new types of efficient cathodes and anodes for solid oxide fuel cells, asymmetric supported oxygen, and hydrogen separation membranes with high permeability and structured catalysts with nanocompositeactive components demonstrating high performance and stability to coking in steam/autothermal reforming of biofuels.

Keywords: Nanocomposites, Synthesis, Solid oxide fuel cells, Supported membranes, Structured catalysts, Biofuels.

Introduction

Production of syngas and pure hydrogen is a key problem in the field of modern hydrogen energy. Design of efficient, inexpensive, and stable to coking catalysts for conversion of biogas and biofuels into syngas and hydrogen, as well as catalytic membrane reactors, is an urgent challenge in the sustainable and renewable energy field [1]. Another related problem is the design of solid oxide fuels cells (SOFCs) that could efficiently generate energy at decreased temperatures from hydrogen, syngas, and biofuels. Hence, mixed ionic-electronic conducting materials for SOFC electrodes and oxygen/hydrogen separation membranes with improved functional properties are to be designed as well.

In this review, recent advances in developing intermediate temperature SOFCs, oxygen and hydrogen separation membranes, and catalysts for the conversion of biofuels into syngas and hydrogen are reviewed. This includes analysis of methods for synthesis of mixed ionic-electronic conducting materials with required enhanced properties, atomic-scale factors controlling their performance and stability, as well as the progress in working characteristics of these devices.

Efficient methods for synthesis of materials

The solid-state reaction and solution combustion synthesis [1-8] are among the most widely used techniques. Intermediate mechanical activation for solid-state reaction helps to obtain highly active precursors allowing the use of short-time calcination [1-3]. A lot of oxide materials were obtained using solution combustion synthesis with different kinds of fuels and chelating agents [4-8]. Pechini technique allows obtaining dispersed powders with uniformity of the element distribution owing to a high level of mixing in a polymerized matrix [9]. Ultrasonic dispersion based on a cavitation effect allows producing fine powders with a low aggregation [1,10].

For dense ceramics, hot pressing [11,12], microwave, and radiation thermal sintering allow decreasing sintering temperatures and processing duration [13-16].

Nanosized catalysts can be obtained using coprecipitation, seeded growth, auto-redox, electrospinning, template methods, one-pot method, wetness impregnation, synthesis in supercritical media, electrophoretic synthesis, and so on. [17-24]. Chemically assisted electrodeposition was developed for highly active electrodes [25] (Figure 1). Hydrothermal [23,26,27] and spray drying [10,28,29] techniques are used as well. During the *in situ* exsolution, metal cations incorporated into the oxide form active metallic nanoparticles on its surface (Figure 2) in reducing atmospheres [30-32].

Novel materials for proton-conducting ceramic fuel cells

It was suggested to use oxides with multicomponent doping (high entropy oxides) for achieving high protonic conductivity. The first protonic conductivity studies of $BaZr_{0.2}Sn_{0.2}Ti_{0.2}Hf_{0.2}Ce_{0.2}O_{3-\delta}$, $BaZr_{0.2}Sn_{0.2}Ti_{0.2}Hf_{0.2}Y_{0.2}O_{3-\delta}$, $BaZr_{1/7}Sn_{1/7}Ti_{1/7}Hf_{1/7}Ce_{1/7}Nb_{1/7}Y_{1/7}O_{3-\delta}$, and $BaZr_{0.15}Sn_{0.15}Ti_{0.15}Hf_{0.15}Ce_{0.15}Nb_{0.15}Y_{0.10}O_{3-\delta}$ were accomplished [33]. The maximal protonic conductivity was achieved for $BaZr_{0.2}Hf_{0.2}Sn_{0.2}Ti_{0.2}In_{0.2}O_3$ (1.5×10^{-4} S/cm at 600 °C). Total conductivity of dense triple-doped solid solutions of barium cerate and zirconate $BaCe_{0.5}Zr_{0.2}Y_{0.1}Yb_{0.1}Gd_{0.1}O_{3-\delta}$ ceramics achieved 1×10^{-2} S/cm at 600 °C in wet air [34].

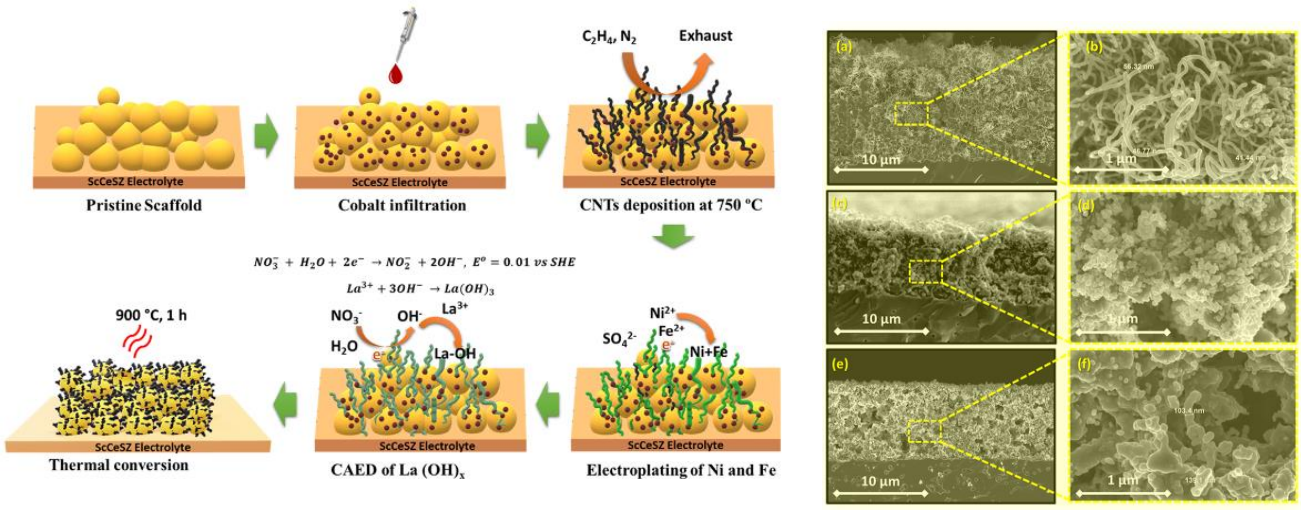

Figure 1. Preparation of nanofibrous composite cathode. Hybrid route including CAED for the preparation of a nanofibrous $LaNi_{0.6}Fe_{0.4}O_3$–$C_{e0.9}Gd_{0.1}O_{1.95}$ (n-LNF-GDC) composite electrode (on the left) and evolution of the electrode microstructure during the process (on the right): (a) a carbon nanotube (CNT)-modified GDC scaffold; (b) a magnified image of the CNTs; (c) Ni–Fe-coated scaffold; (d) a magnified image of Ni–Fe coating; (e) a nanofibrous n-LNF−GDC cathode calcined at 900 °C; and (f) magnified image of the n-LNF−GDC cathode [19]. CAED, chemically assisted electrodeposition.

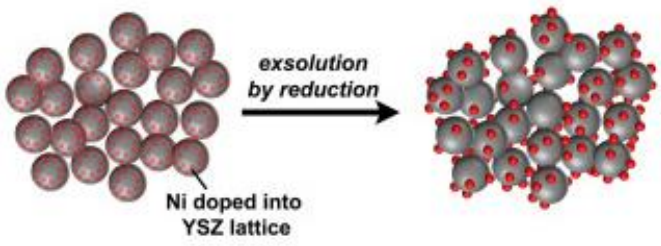

Figure 2. Demonstration of nickel exolution effect [30].

High entropy BIMEVOXes are based on the parent $Bi_4V_2O_{11}$ with vanadium partially replaced by several metals [35]. Ionic conductivity of high entropy BIMEVOX is comparable to those for single-doped BIMEVOXes, they have an increased stability and the highest ionic transference numbers.

For calcium-doped layered perovskites $BaNd_{1-x}Ca_xInO_{4-x/2}$, total conductivity was 1-2 orders of magnitude higher than that for $BaNdInO_4$ [36].

Isotope exchange of oxygen

$^{18}O_2$ is commonly used for studying the oxygen mobility. However, oxygen substitution is often limited by oxygen dissociation on the surface, hence, lowering sensitivity to diffusion. A high surface exchange rate with $C^{18}O_2$ allows a comprehensive elucidation of the diffusion features. For $C^{18}O_2$ exchange with $PrNi_{0.5}Co_{0.5}O_3$, the response curve has two extrema (Figure 3) making evidence of at least two forms of oxygen in the bulk, whereas the fastest oxygen form is not discovered during the experiment with $^{18}O_2$. Such nonuniformity was found for most oxides, and composites and models were suggested to describe it [37-40].

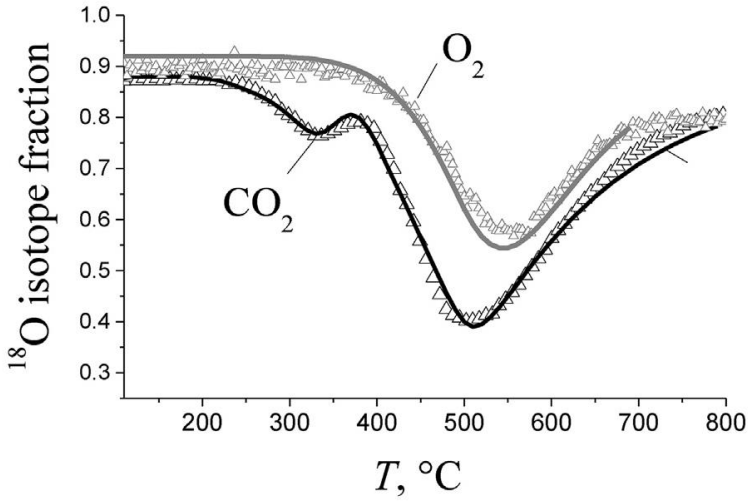

Figure 3. Temperature-programmed exchange with $^{18}O_2$ and $C^{18}O_2$ on $PrNi_{0.5}Co_{0.5}O_{3-\delta}$ in the flow reactor. Points — experiment, lines — calculation [37,38].

Symmetrical solid oxide fuel cells

Promising direction in SOFC technology is the development of symmetrical cells (SSOFCs) with two identical electrodes. The use of the same material for oxygen and fuel electrodes improves chemical and thermal compatibility of the cell components and contributes to simplification and cost-effectiveness of the fabrication process [41-44].

$Sr_2Fe_{1.5}Mo_{0.5}O_{6-\delta}$ (SFM) was proposed as a prospective symmetrical electrode material. The SFM was studied in oxidizing atmospheres to clarify kinetics of oxygen reduction and hydrogen oxidation in the anode conditions, as well as during redox cycling in an SSOFC [45-49]. Electrochemical activity of $Sr_{1.95}Fe_{1.4}Ni_{0.1}Mo_{0.5}O_{6-\delta}$ electrodes was higher than that of SFM in both oxidizing and reducing atmospheres, which can be explained by exsolution of nickel particles having high electrocatalytic activity [50,51].

The $Pr_2NiO_{4+\delta}$ catalyst effectively increases the rates of oxygen reduction and hydrogen oxidation. The rate of oxygen reduction after its introduction into the cathode increases owing to increase in the rate of oxygen exchange, whereas the enhanced rate of hydrogen oxidation is provided by the increased rate of its adsorbed molecule dissociation (Figure 4) [49].

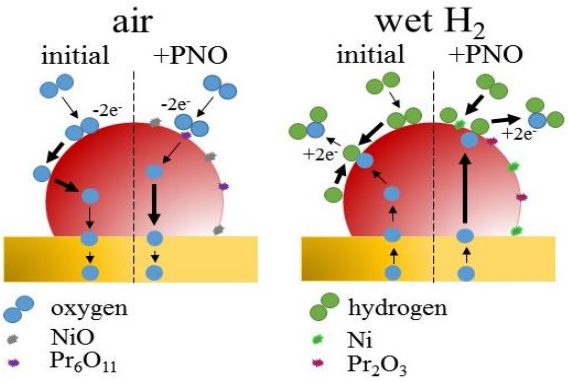

Figure 4. The pathways for oxygen reduction and hydrogen oxidation reactions before and after impregnation with the PNO catalyst [49]. PNO, $Pr_2NiO_{4+\delta}$.

The application of this design to proton ceramic cells is only at the beginning of its development. New $Nd_{1-x}Ba_xFe_{0.9}M_{0.1}O_{3-\delta}$ materials (M = Cu, Ni; x = 0.4, 0.6) were investigated [52]. The reported results are among the first concerning the effective electrode operation in SSOFC's with proton-conducting electrolytes.

Reversible solid oxide cells

Reversible solid oxide cells are promising electrochemical devices which can function effectively both in the fuel cell and electrolysis mode [53,54]. The reversible solid oxide cells based on proton ceramic (rPCC) with a $BaCe_{0.5}Zr_{0.3}Y_{0.1}Yb_{0.1}O_{3-\delta}$ membrane generated a maximal power density and a hydrogen evolution rate. This complex approach allowed the main factors influencing the rPCC performance to be disclosed, and some approaches were proposed for future rPCCs' optimization. Because the ohmic resistance exceeds 50% of the total rPCCs' resistance in all studied modes, achievement of the next generation of cells operating below 600 °C with high performance and efficiency can be implemented through decreasing the electrolyte thickness to the 1-5 μm range [55-59].

Solid oxide fuel cell anodes

Metallic nickel in Ni-YSZ anodes serves as a catalyst for fuel oxidation and provides a path for electronic conduction. It is not suitable for hydrocarbon-fueled SOFCs because Ni catalyzes hydrocarbons cracking resulting in coking and also suffers from poisoning by sulfur and other contaminants. Significant efforts have been dedicated to the development of vanadium- and molybdenum-based components. Increasing Mo fraction in Ni-Mo catalysts significantly improves resistance to coking although reduces catalytic activity [60]. The Ni(11 wt.%)-Mo(3 wt.%)-YSZ reforming layer at the Ni-YSZ anode ensured a stable performance of the isooctane-fueled cell, whereas a similar cell without a reforming layer failed after 12 h [61]. The addition of molybdenum to the $Ni\text{-}Ce_{0.5}Zr_{0.5}O_2$ anode improved the electrical conductivity, nearly doubled power density, and ensured a stable operation [62]. The long-term (1737 h) stable performance of a cell with the $Ni\text{-}Mo\text{-}CeO_2$ anode fueled by H_2S and siloxane-contaminated biogas was demonstrated [63].

Perovskite-type AVO_3 and $AMoO_3$ (A = Ca, Sr) oxides attracted attention as prospective ceramic components owing to their high electronic conductivity under reducing conditions. Increasing molybdenum content in the B-sublattice of $CaV_{1-x}Mo_xO_{3-\delta}$ increases electrical conductivity and reduces thermal expansion [64]. Materials were stable in the pO_2 range corresponding to operation conditions but undergo oxidative decomposition at higher pO_2. A partial substitution by transition metal with a more stable oxidation state can extend the stability domain. A compromise between a high electrical conductivity of $SrVO_3$ and thermodynamic stability of $SrTiO_3$ was demonstrated for $SrV_{1-y}Ti_yO_{3-\delta}$ [65]. Note the difference in the thermodynamic stability of V- and Mo-based perovskites under highly reducing conditions. Easier reducible molybdenum tends to exsolve at temperatures ≥1000 °C [64,66], whereas vanadium cations remain in a mixed 3+/4+ oxidation state even at 1500 °C [64].

$SrMo_{0.5}Ti_{0.5}O_{3-\delta}$ exhibits higher conductivity than that of the V-based counterpart [67]. This material showed good compatibility with electrolytes, good coking resistance, and sulfur tolerance [67]. The electrochemical activity of $SrMo_{0.5}Ti_{0.5}O_{3-\delta}$ can be improved by providing a minor cation deficiency in the B-sublattice [68]. The power density of cells with $Sr(Mo,Ti)O_{3-\delta}$ anodes fueled by H_2S-contaminated syngas can be increased ~2 times by the surface modification with Pd [67,68].

Oxidized $SrV_{0.5}Mo_{0.5}O_4$ can be easily reduced to highly conductive $SrV_{0.5}Mo_{0.5}O_{3-\delta}$ [69]. The reduction of the nickel-doped $SrV_{0.5}Mo_{0.5}Ni_{0.1}O_{4-\delta}$ precursor leads to exsolution of nickel covering the surface of perovskite: this results in the increase in electrical conductivity; a decrease in the electrode polarization resistance; a good electrocatalytic activity in H_2S-contaminated and hydrocarbon fuels; as well as a stable performance [69].

Asymmetric supported oxygen and hydrogen separation membranes

Conventional oxygen and hydrogen separation membranes consist of perovskites and noble metals or their alloys, respectively, lacking stability [1,38]. Using nanocomposites can help to avoid such drawbacks. Membranes based on $PrNi_{0.5}Co_{0.5}O_3$ - $Ce_{0.9}Y_{0.1}O_2$, $La_{0.3}Bi_{0.7}MnO_{3+\delta}$ – $Bi_{1.5}Y_{0.3}Sm_{0.2}O_2$, and $La_{5.5}WO_{11.25-\delta}$ - NiCu - demonstrated high oxygen/hydrogen permeation fluxes and stable performance in catalytic reactions [1,38,70,71].

Structured catalysts with nanocomposite-active components for biogas and biofuel conversion into syngas and hydrogen

The main problem for catalysts for biofuel reforming, especially for the methane dry reforming, is coking leading to deactivation, especially for those composed of inexpensive Ni on different supports [72-75]. The most efficient approaches to deal with this problem are based on the next concepts of design:

1. Suppress acidity of supports responsible for catalysis of reactions leading to coking.

2. Use oxide supports with a high oxygen mobility and reactivity containing transition and/or rare-earth cations reduced in the reaction conditions and able to activate carbon dioxide on the oxygen vacancies generating reactive oxygen species rapidly migrating to the metal-oxide interface and interacting with the activated fragments of fuels converting them into syngas.

3. Provide a strong metal-support interaction, which prevents metal sintering in the reaction conditions and ensures developed metal-support interface.

4. Use bimetallic catalysts, the best Ru-Ni alloy nanoparticles to prevent carbon nucleation.

5. Use supports with a core-shell structure (mesoporous $MgAl_2O_4$ with supported layers of perovskite, fluorite, or spinel oxides with high oxygen mobility and reactivity) to increase surface area, porosity, and thermal stability of catalysts.

6. Use heat-conducting substrates to support active components, thus providing efficient heat and mass transfer in the reactors.

Doping of alumina with Mg indeed effectively suppresses acidity (increases proton affinity) as demonstrated by the analysis of the shift of hydroxyls infra-red (IR) bands owing to CO adsorption [76]. This results in a higher stability of Ni-containing catalysts on these supports in the reactions of methane [72-77], ethanol [76], and other biofuels (glycerol, ethylacetate, and so on) [76,78] reforming owing to coking suppression.

For Ni catalysts on oxide supports with perovskite, fluorite, and spinel structures containing cations able to change their charge state in the reaction conditions (Mn, Cr, Fe, Pr, Ce, and so on), coking was suppressed owing to their high oxygen mobility and reactivity [75,76,79-83]. For such catalysts, the independent activation of reagents was reliably demonstrated by pulse experiments (including temporal analysis of products (TAP) pulse responses and pulse microcalorimetry) and SSITKA, steady state isotope transient kinetic analysis [75,80,84]. Estimation of oxygen self-diffusion coefficients for these catalysts demonstrated their high values providing a fast oxygen transport to the metal-support interface [75,80]. At the same time, for $Ni/La_2Zr_2O_7$ catalyst without cations of variable charges in the support, SSITKA revealed that oxygen of the support is not involved in the methane dry reforming [85].

The most reliable method to characterize the metal/support interaction is Fourier-transformed infrared spectroscopy of the adsorbed CO [75,76,80]. Small sizes of metal particles owing to strong interaction with a support, their decoration by oxidic fragments, as well as the presence on the surface of metal alloy nanoparticles, atoms of each type mainly surrounded by atoms of another type results in domination in Fourier-transformed infrared spectroscopy spectra of adsorbed CO bands corresponding to terminal carbonyls (νCO 2000-2100 cm^{-1}), whereas bands corresponding to CO adsorbed on neighboring atoms of the same type (bridging carbonyls, $\nu CO < 2000$ cm^{-1}) disappear. Domination of terminal carbonyls and a high intensity of their bands correlates with a high catalytic activity and coking stability of catalysts with Ni-Ru nanoparticles loaded on bulk fluorite, spinel and perovskite oxides [75,80], or Mg-doped alumina covered with their layers [76]. This is explained by prevention of carbon fragment nucleation on isolated Ni atoms and by suppression of carbon diffusion into the bulk of metal alloy particles, thus avoiding carbon nanotube nucleation at the metal-support interface [72,77].

Because catalysts based on bulk oxides with spinel, fluorite, and perovskite structure possessing a high oxygen mobility and reactivity have in general much lower specific surface area as compared with traditional supports (γ-Al_2O_3 and so on), a lot of work was devoted to design of core-shell structures by supporting reactive oxide layers on high surface area supports [75,76,78,84,86]. The most efficient combination was found to be mesoporous $MgAl_2O_4$ with supported layers of $Ce_{0.35}Zr_{0.35}Pr_{0.3}O_2$ fluorite promoted by Ru + Ni nanoparticles owing to optimized interaction between components, only moderately decreasing the reactive surface oxygen content and increasing its bonding strength [76,84].

Use of the ethylendiaminetetraacetic acid, EDTA-chelating agent in Ni supporting by impregnation on a ceria-loaded $MgAl_2O_4$ improved catalysts activity and stability in ethanol steam reforming owing to stronger metal-support interaction [78]. However, application of acetylacetone to load Ru + Ni on the mesoporous $MgAl_2O_4$ support precovered by $Ce_{0.35}Zr_{0.35}Pr_{0.3}O_2$ or to load $PrNi_{0.9}Ru_{0.1}O_3$ on a pure $MgAl_2O_4$ support resulted in excessively strong incorporation of Ni and Ru into support, hence, decreasing catalytic activity [76]. Hence, preparation procedures are to be optimized with a due regard for interaction of active components with the support at the impregnation step. Thus, for 50 wt.% $Pr_{0.15}Sm_{0.15}Ce_{0.35}Zr_{0.35}O_2$ + 50 wt.% $LaMn_{0.45}Ni_{0.45}Ru_{0.1}O_3$, nanocomposite formation of the perovskite phase from a polyester matrix with dispersed fluorite oxide provides the nanocomposite with a high specific surface area, developed interphases, and a high activity in EtOH (ethanol) reforming. In a one-pot synthesis method from a polyester containing all cations, the perovskite phase was not formed owing to La incorporation into the fluorite matrix, hence, a lower activity was demonstrated [81].

For any practical application, catalysts for conversion of biofuels into syngas are to be supported as thin layers on monolithic substrates, which allows minimization or even elimination of any heat and mass transfer limitations typical for granulated catalysts [75,76,87]. Supporting thin layers of active components based on a mesoporous $MgAl_2O_4$ support loaded with Ru + Ni/$Ce_{0.35}Zr_{0.35}Pr_{0.3}O_2$ on a FeCr alloy honeycomb substrate allowed to provide a stable performance and high yields of syngas in dry reforming of natural gas, steam reforming of ethanol, and oxy-steam reforming of ethylacetate at contact times several times lower than for catalysts on the same substrate loaded with catalysts based on bulk-doped Ce-Zr-O fluorite or traditional alumina supports [75,76].

Conclusions and outlook

New methods of materials synthesis for SOFC, permselective membranes, and catalysts for biofuel conversion apparently open the ways to improve their functional properties and achieve required characteristics of devices constructed on their bases. Though additional research is clearly required, especially in the case of SOFCs with proton-conducting electrolytes, the progress made in the last two years is apparent. From the fundamental point of view, the most important are results related to design of mixed ionic-electronic conductors via multiple doping or preparation of nanocomposites with a core-shell structure. Among the characterization methods, a great progress was achieved in the oxygen isotope exchange methods for estimation of oxygen self-diffusion coefficients and SSITKA to elucidate kinetic features of catalytic reactions.

Funding

This work was supported by the AAAA-A21-121011390007-7 budget project of the Boreskov Institute of catalysis. A.A.Y. gratefully acknowledges financial support within the project CICECO - Aveiro Institute of Materials (UIDB/50011/2020 and UIDP/50011/2020) financed by national funds through the FCT/MCTES and when appropriate cofinanced by FEDER under the PT2020 Partnership Agreement.

References

Papers of particular interest, published within the period of review, have been highlighted as: * of special interest

* [1] V.A. Sadykov, N.F. Eremeev, Y.E. Fedorova, A.V. Krasnov, L.N. Bobrova, Y.N. Bespalko, A.I. Lukashevich, P.I. Skriabin, O.L. Smorygo, A.C. Van Veen, Design and performance of asymmetric supported membranes for oxygen and hydrogen separation, Int. J. Hydrog. Energy 46(3) (2021) 20222-20239. https://doi.org/10.1016/j.ijhydene.2020.01.106.

A review devoted to synthesis and studies of various nanocomposite materials for gas separation membranes.

[2] A. López-Vergara, L. Vizcaíno-Anaya, J.M. Porras-Vázquez, G. Baldinozzi, L. dos Santos-Gómez, J. Canales-Vazquez, D. Marrero-López, E.R. Losilla, Unravelling crystal superstructures and transformations in the $La_{6-x}MoO_{12-\delta}$ ($0.6 \leq x \leq 3.0$) series. A system with tailored ionic/electronic conductivity, Chem. Mater. 59 (2020) 1444-1452. https://doi.org/10.1021/acs.chemmater.0c02673.

* [3] I.V. Kolbanev, A.V. Shlyakhtina, E.N. Degtyarev, E.Yu. Konysheva, N.V. Lyskov, D.N. Stolbov, A.N. Streletskii, Room-temperature mechanochemical synthesis of RE molybdates: impact of structural similarity and basicity of oxides, J. Am. Cer. Soc. 00 (2021) 1-13. https://doi.org/10.1111/jace.17939.

Dissolving molybdenum oxide in rare earth element oxide occurs already during mechanical activation at room temperature leading to synthesis of molybdate with the same structure as that of initial rare earth element oxide. As a result, La molybdate forms having the structure of low-temperature lanthanum oxide La_2O_3 ($P\bar{3}m1$, no. 164); the other rare earth element (Dy – Yb, Y) molybdates exist having bixbyite structure as well as the initial Ln_2O_3 oxides ($Ia\bar{3}$, no. 206), while samarium and gadolinium molybdates have Sm_2O_3 structure (*C2/m*, no. 12)

[4] E. Carlos, R. Martins, E. Fortunato, R. Branquinho, Solution combustion synthesis: towards a sustainable approach for metal oxides, Chem. Eur. J. 26(42) (2020) 9099-9125. https://doi.org/10.1002/chem.202084264.

[5] M. Khaliulin, A.A. Koshkina, Influence of fuel on phase formation, morphology, electric and dielectric properties of iron oxides obtained by SCS method, Ceram. Int. 47 (2021) 11942-11950. https://doi.org/10.1016/j.ceramint.2021.01.035.

[6] T.S. Cam, T.A. Vishnevskaya, S.O. Omarov, V.N. Nevedomsky, V.I. Popkov, Urea-nitrate combustion synthesis of CuO/CeO_2 nanocatalysts toward low-temperature oxidation of CO: the effect of Red/Ox ratio, J. Mater. Sci. 55 (2020) 11891-11906. https://doi.org/10.1007/s10853-020-04857-3.

[7] A.S. Urusova, M.Yu. Mychenko, A. Maignan, V.A. Cherepanov, Conductivity and stability of ceramic $Sr_{1-x}Y_xFeO_{3-\delta}$ solid solutions, Ceram. Int. 46(15) (2020) 24718-24722. https://doi.org/10.1016/j.ceramint.2020.06.262.

[8] O.V. Komkova, S.A. Mukha, A.M. Ozerova, G.V. Odegova, V.I. Simagina, O.A. Bulavchenko, A.V. Ishchenko, O.V. Netskina, The formation of perovskite during the combustion of an energy-rich glycine-nitrate precursor, Materials 13(22) (2020) 5091. https://doi.org/10.3390/ma13225091.

* [9] S. Sharma, M.K. Verma, N.D. Sharma, N. Choydhary, S. Singh, D. Singh, Rare-earth doped Ni-Co ferrites synthesized by Pecchini method: Cation distribution and high temperature magnetic studies, Ceram. Int. 47(12) (2021) 17510-17519. https://doi.org/10.1016/j.ceramint.2021.03.069.

* [10] V.A. Sadykov, M.N. Simonov, Y.N. Bespalko, L.N. Bobrova, N.F. Eremeev, M.V. Arapova, E.A. Smal', N.V. Mezentseva, S.N. Pavlova, Design and characterization of nanocomposite catalysts for biofuel conversion into syngas and hydrogen in structured reactors and membranes, Kinet. Catal. 60(5) (2019) 582-605. https://doi.org/10.1134/S0023158419050082.

Characteristics of nanomaterials prepared by Pecchini method and solvothermal method in supercritical alcohols are compared.

[11] V.-H. Nguyen, S.A. Delbari, M.S. Asl, A.S. Namini, M.G. Kakroudi, Y. Azizian-Kalandaragh, Q. Van Le, M. Mohammadi, M. Shokouhimehr, Role of hot-pressing temperature on densification and microstructure of ZrB2–SiC ultrahigh temperature ceramics, Int. J. Refract. Hard. Met. 93 (2020) 105355. https://doi.org/10.1016/j.ijrmhm.2020.105355.

[12] D.A. Permin, S.S. Balabanov, I.L. Snetkov, O.V. Palashov, A.V. Novikova, O.N. Klyusik, I.V. Ladenkov, Hot pressing of $Yb:Sc_2O_3$ laser ceramics with LiF sintering aid, Opt. Mater. 100 (2020) 109701. https://doi.org/10.1016/j.optmat.2020.109701.

[13] K.I. Rybakov, S.V. Egorov, A.G. Eremeev, V,V. Kholoptsev, I.V. Plotnikov, A,A. Sorokinm Ultra-rapid microwave sintering employing thermal instability and resonant absorption, J. Mater. Res. 34 (2019) 2620–2634. https://doi.org/10.1557/jmr.2019.232.

[14] T. Garnault, D. Bouvard, J.-M. Chaix, S. Marinel, C. Harnois, Is direct microwave heating well suited for sintering ceramics?, Ceram. Int. 47(12) (2021) 16716-16729. https://doi.org/10.1016/j.ceramint.2021.02.242.

[15] A.S. Klimov, I.Y. Bakeev, E.M. Oks, V.T. Tran, A.A. Zenin, Electron beam sintering of gradient Al_2O_3-ZrO_2 ceramics with the forevacuum plasma electron source, J. Phys.: Conf. Ser. 1488 (2020) 012010.

[16] A.S. Klimov, I.Y. Bakeev, E.M. Oks, A.A. Zenin, Electron-beam sintering of an Al_2O_3/Ti composite using a forevacuum plasma-cathode electron source, Ceram. Int. 46(14) (2020) 22276-22281. https://doi.org/10.1088/1742-6596/1488/1/012010.

[17] W. Yang, X. Wang, S. Song, H. Zhang, Synthesis and application of noble-metal-free CeO_2-based mixed-oxide nanocatalysts, Chem 5(7) (2019) 1743-1774. https://doi.org/10.1016/j.chempr.2019.04.009.

[18] T. Wang, Y. Nakagawa, M. Tamura, K. Okumura, K. Tomishige, Tungsten–zirconia-supported rhenium catalyst combined with a deoxydehydration catalyst for the one-pot synthesis of 1,4-butanediol from 1,4-anhydroerythritol, React. Chem. Eng. 5(7) (2020) 1237-1250. https://doi.org/10.1039/D0RE00085J.

[19] L. Wolski, G. Nowaczyk, S. Jurga, M. Ziolek, Influence of co-precipitation agent on the structure, texture and catalytic activity in low-temperature oxidation of benzyl alcohol, Catalysts 11 (2021) 641. https://doi.org/10.3390/catal11050641.

[20] S. Asaithambi, P. Sakthivel, M. Karruppaiah, R. Yuvakkumar, K. Balamurugan, T. Ahamad, M.A. Majeed Khan, G. Ramalingam, Mustafa K.A. Mohammed, G. Ravi, Preparation of Fe-SnO_2@CeO_2 nanocomposite electrode for asymmetric supercapacitor device performance analysis, J. Energy Stor. 36 (2021) 102402. https://doi.org/10.1016/j.est.2021.102402.

* [21] E.Yu. Pikalova, E.G. Kalinina, Solid oxide fuel cells based on ceramic membranes with mixed conductivity: improving efficiency, Russ. Chem. Rev. 90 (2021) 703 https://doi.org/10.1070/RCR4966.

The approaches to increasing the efficiency of solid-oxide fuel cells based on electrolytic membranes are reviewed. The materials science concepts, various technological approaches and mathematical modelling are considered. The special attention is paid to using ceria based electrolytes.

* [22] J.W. Annis, J.M. Fisher, D. Thompsett, R.I. Walton, Solvothermal synthesis routes of substituted cerium dioxide materials, Inorganics 9(6) (2021) 40.1 https://doi.org/10.3390/inorganics9060040.

The novel solvothermal and hydrothermal techniques for synthesis of complex oxides and solid solutions based on the use of supercritical water, alcohols, carbon dioxide and etc. allow to carry out the process in continuous and scalable conditions resulting in obtaining nanostructures (particles, roads, flakes etc.) at relatively low temperatures

[23] E.G. Kalinina, D.S. Rusakov, E.Yu. Pikalova, Electrophoretic deposition of coatings and bulk compacts using magnesium-doped aluminium oxide nanopowders, Chem. Tech. Acta 8(2) (2021) 20218206. https://doi.org/10.15826/chimtech.2021.8.2.06.

* [24] P. Qu, S. Wang, W. Hu, Y. Wu, J. Chen, G. Zhang, P. Shen, Y. Chen, L. Zhong, A novel strategy to design PtPd bimetallic catalysts for efficient methane combustion, Catal. Commun. 135 (2020) 105900. https://doi.org/10.1016/j.catcom.2019.105900.

Wetness impregnation method is based on the incipient wetness impregnation of the oxide, solid solution or nanocomposite supports with soluble precursor of active component. This method allows to synthesized bulk and mesoporous catalysts. The main disadvantage of the infiltration technique is that the process is time-consuming due to multiple infiltration and calcination steps.

[25] A. Shaur, S. U. Rehman, H.-S. Kim, R.-H. Song, T.-H. Lim, J.-E. Hong, S.-J. Park, S.-B. Lee, Hybrid electrochemical deposition route for the facile nanofabrication of Cr-poisoning-tolerant La(Ni,Fe)$O_{3-\delta}$ cathode for solid oxide fuel cells, ACS Appl. Mater. Interfaces 12(5) (2020) 5730–5738 https://doi.org/10.1021/acsami.9b17807.

[26] M. Liao, C. Guo, W. Guo, T. Hu, J. Xie, P. Gao, H. Xiao, One-step growth of CuO/ZnO/CeO_2/ZrO_2 nanoflowers catalyst by hydrothermal method on Al_2O_3 support for methanol steam reforming in a microreactor, Int. J. Hydrog. Energy 46(14) (2021) 9280-9291. https://doi.org/10.1016/j.ijhydene.2020.12.116.

* [27] S.F. Tikhov, T.P. Minyukova, K.R. Valeev, S.V. Cherepanova, A.N. Salanov, N.V. Shtertser, V.A. Sadykov, Design of ceramometal $CuFeAlO_x$/CuFeAl composites and their catalytic potential for water gas shift reaction, Mater. Chem. Phys. 221 (2019) 349-355. https://doi.org/10.1016/j.matchemphys.2018.09.041.

Hydrothermal method is based on processing of the catalyst precursors (oxides, alloys, etc.) in water or water solution to obtain highly dispersed nanosized catalyst. This technique prevents self-propagating high temperature synthesis, preserves the mesoporous structure of the oxide layer and allows to synthesize cermets of various geometrical shapes.

[28] N.P. de Moraes, R.B. Anselmo, L.O. Sartor, G.V.J. Dantas, L.A. Rodrigues, L.C. e Carvalho, Spray drying as feasible processing technique to enhance the photocatalytic activity of the Nb_2O_5/carbon xerogel composite, Mater. Lett. 273 (2020) 127932. https://doi.org/10.1016/j.matlet.2020.127932.

[29] C. Yao, H. Xu, A. Li, J. Li, F. Pang, P. Zhao, J. He, W. Yi, Y. Jiang, L. Huang, Synthesis of PtCoNiRu/C nanoparticles by spray drying combined with reduction sintering for methanol electro-oxidation, RSC Adv. 10 (2020) 3579-3587. https://doi.org/10.1039/C9RA09764C.

[30] S. Joo, C. Lim, O. Kwon, L. Zhang, J. Zhou, J.-Q. Wang, H.Y. Jeong, Y.-W. Sin, S. Choi, G.Kim, The first observation of Ni nanoparticle exsolution from YSZ and its application for dry reforming of methane, Materials Reports: Energy 1(2) 2021 100021. https://doi.org/10.1016/j.matre.2021.100021.

[31] D.J. Deka, J. Kim, S. Gunduz, M. Aouine, J.-M.M. Millet, A.C. Co, U.S. Ozkan, Investigation of hetero-phases grown via in-situ exsolution on a Ni-doped (La,Sr)FeO_3 cathode and the resultant activity enhancement in CO_2 reduction, Appl. Catal. B Environ. 286 (2021) 119917, https://doi.org/10.1016/j.apcatb.2021.119917.

[32] L. Thommy, M. Benamira, T. Jardiel, V. Günes, O. Joubert, M.T. Caldes, Ru exsolution in substituted $La_{0.75}Sr_{0.25}Cr_{0.5}Mn_{0.5}O_{3-\delta}$ compound as anode material for an IT-SOFCs, Materi. Chem. Phys. 268 (2021) 124724 https://doi.org/10.1016/j.matchemphys.2021.124724.

[33] M. Gazda, T. Miruszewski, D. Jaworski, A. Mielewczyk-Gryń, W. Skubida, S. Wachowski, P. Winiarz, K. Dzierzgowski, M. Łapiński, I. Szpunar, E. Dzik, Novel class of proton conducting materials – high entropy oxides, ACS Materials Lett. 2(10) 2020, 1315–1321. https://doi.org/10.1021/acsmaterialslett.0c00257.

[34] S. Rajendran, N. K. Thangavel, H. Ding, Y. Ding, D. Ding, L. M. Reddy Arava, Tri-doped $BaCeO_3$-$BaZrO_3$ as a chemically stable electrolyte with high proton-conductivity for intermediate temperature solid oxide electrolysis cells (SOECs). ACS Appl. Mater. Interfaces 12 (2020) 38275−38284. https://doi.org/10.1021/acsami.0c12532.

[35] A. Dziegielewska, M. Malys, W. Wrobel, S. Hull, Y. Yue, F. Krok, I. Abrahams, $Bi_2V_{1-x}(Mg_{0.25}Cu_{0.25}Ni_{0.25}Zn_{0.25})_xO_{5.5-3x/2}$: A high entropy dopant BIMEVOX, Solid State Ionics 60 (2021) 115543. https://doi.org/10.1016/j.ssi.2020.115543.

[36] Zhou Y, Shiraiwa M, Nagao M, Fujii K, Tanaka I, Yashima M, Baque L, Basbus JF, Mogni LV, Skinner SJ: Protonic conduction in the BaNdInO4 structure achieved by acceptor doping. Chem Mater 2021, 33:2139–2146. https://doi.org/10.1021/acs.chemmater.0c04828.

[37] V.A. Sadykov, E.M. Sadovskaya, N.F. Eremeev, P.I. Skriabin, A.V. Krasnov, Y.N. Bespalko, S.N. Pavlova, Y.E. Fedorova, E.Y. Pikalova, A.V. Shlyakhtina, Oxygen mobility in the materials for solid oxide fuel cells and catalytic membranes (Review), Russ. J. Electrochem. 55(8) (2019) 701-718. https://doi.org/10.1134/S1023193519080147.

* [38] V.A. Sadykov, E.M. Sadovskaya, N.F. Eremeev, E.Y. Pikalova, N.M. Bogdanovich, E.A. Filonova, T.A. Krieger, Y.E. Fedorova, A.V. Krasnov, P.I. Skriabin, A.I. Lukashevich, R. Steinberger-Wilckens, I.C. Vinke, Novel materials for solid oxide fuel cells cathodes and oxygen separation membranes: fundamentals of oxygen transport and performance, Carbon Resources Conversion 3 (2020) 112-121. https://doi.org/10.1016/j.crcon.2020.08.002.

Relation between performance of these devises and oxygen mobility of materials estimated by temperature-programmed oxygen exchange with $C^{18}O_2$ was analyzed.

* [39] V.A. Sadykov, E.M. Sadovskaya, E.A. Filonova, N.F. Eremeev, V.D. Belyaev, V.A. Tsvinkinberg, E.Y. Pikalova, Oxide ionic transport features in Gd-doped La nickelates, Solid State Ionics 357 (2020) 115462:1-8. https://doi.org/10.1016/j.ssi.2020.115462.

The model for Gd-doped La nickelates included one fast diffusion channel involving the most mobile oxygen atoms and subsequent isotope exchange with less mobile neighboring atoms

* [40] V. Sadykov, A. Shlyakhtina, N. Lyskov, E. Sadovskaya, S. Cherepanova, N. Eremeev, V. Skazka, V. Goncharov, E. Kharitonova, Oxygen diffusion in Mg-doped Sm and Gd zirconates with pyrochlore structure, Ionics 26(9) (2020) 4621-4633. https://doi.org/10.1007/s11581-020-03614-5.

For Mg-doped Sm and Gd zirconates two-dimensional model considering the fast diffusion along grain boundaries and diffusion within the grains' bulk was suggested

[41] S.Y. Istomin, N.V. Lyskov, G.N. Mazo, E.V. Antipov, Electrode materials based on complex d-metal oxides for symmetrical solid oxide fuel cells, Russ. Chem. Rev. 90 (2021) 644–676. https://doi.org/10.1070/RCR4979.

[42] X. Peng, Y. Tian, Y. Liu, W. Wang, J. Chen, J. Li, B. Chi, J. Pu, J. Li, A double perovskite decorated carbon-tolerant redox electrode for symmetrical SOFC, Int. J. Hydrog. Energy 45 (2021) 14461–14469. https://doi.org/10.1016/j.ijhydene.2020.03.151.

[43] M.B. Hanif, J. Gao, K. Shaheen, Y. Wang, M. Yasir, C. Li, C. Li, Highly active and novel A-site deficient symmetric electrode material $(Sr_{0.3}La_{0.7})_{1-x}(Fe_{0.7}Ti_{0.3})_{0.9}Ni_{0.1}O_{3-\delta}$ and its effect on electrochemical performance of SOFCs, Int. J. Hydrogen Energy 46 (2021) 8778-8791. https://doi.org/10.1016/j.ijhydene.2020.12.093.

[44] L. Santos-Gómez, J.M. Porras-Vázquez, E.R. Losilla, D. Marrero-López, P.R. Slater, Investigation of PO43− oxyanion-doping on the properties of $CaFe_{0.4}Ti_{0.6}O_{3-\delta}$ for potential application as symmetrical electrodes for SOFCs, J. Alloys and Comp. 835 (2020) 155437. https://doi.org/10.1016/j.jallcom.2020.155437.

[45] D.A. Osinkin, Kinetics of CO oxidation and redox cycling of $Sr_2Fe_{1.5}Mo_{0.5}O_{6-\delta}$ electrode for symmetrical solid state electrochemical devices, J. Power Sources 418 (2019) 17–23. https://doi.org/10.1016/j.jpowsour.2019.02.026.

[46] Y. Zhang, Z. Zhu, Y. Gu, H. Chen, Y. Zheng, L. Ge, Effect of Cl doping on the electrochemical performance of $Sr_2Fe_{1.5}Mo_{0.5}O_{6-\delta}$ cathode material for solid oxide fuel cells, Ceram. Int. 46 (2020) 22787–22796. https://doi.org/10.1016/j.ceramint.2020.06.046.

[47] D.A. Osinkin, A.A. Kolchugin, N.M. Bogdanovich, S.M. Beresnev, Performance and redox stability of a double–layer $Sr_2Fe_{1.5}Mo_{0.5}O_{6-\delta}$ – based electrode for solid state electrochemical application. Electrochim. Acta 361 (2020) 137058. https://doi.org/10.1016/j.electacta.2020.137058.

[48] J. Gao, Y. Zhang, X. Wang, L. Jia, H. Jiang, M. Huang, A. Toghan, Nitrogen-doped $Sr_2Fe_{1.5}Mo_{0.5}O_{6-\delta}$ perovskite as an efficient and stable catalyst for hydrogen evolution reaction, Mat. Today. Sci. 20 (2021) 100695. https://doi.org/10.1016/j.mtener.2021.100695.

[49] D.A. Osinkin, Precursor of $Pr_2NiO_{4-\delta}$ as a highly effective catalyst for the simultaneous promotion of oxygen reduction and hydrogen oxidation reactions in solid oxide electrochemical devices, Int. J. Hydrogen Energy 46 (2021) 24546–24554. https://doi.org/10.1016/j.ijhydene.2021.05.022.

[50] X. Meng, Y. Wang, Y. Zhao, T. Zhang, N. Xu, X. Chen, M. Miao, T. Liu, In-situ exsolution of nanoparticles from Ni substituted $Sr_2Fe_{1.5}Mo_{0.5}O_6$ perovskite oxides with different Ni doping contents, Electrochim. Acta 348 (2020) 136351. https://doi.org/10.1016/j.electacta.2020.136351.

[51] D.A. Osinkin, E.P. Antonova, K.S. Shubin, N.M. Bogdanovich, Influence of nickel exsolution on the electrochemical performance and rate-determining stages of hydrogen oxidation on $Sr_{1.95}Fe_{1.4}Ni_{0.1}Mo_{0.5}O_{6-\delta}$ promising electrode for solid state electrochemical devices, Electrochim. Acta 369 (2021) 137673. https://doi.org/10.1016/j.electacta.2020.137673.

[52] L.R. Tarutina, J.G. Lyagaeva, A.S. Farlenkov, A.I. Vylkov, G.K. Vdovin, A.A. Murashkina, A.K. Demin, D.A. Medvedev, Doped (Nd,Ba)FeO_3 oxides as potential electrodes for symmetrically designed protonic ceramic electrochemical cells, J. Solid State Electrochem. 24 (2020) 1453–1462. https://doi.org/10.1007/s10008-020-04522-4.

[53] M.B. Mogensen, M. Chen, H.L. Frandsen, C. Graves, J.B. Hansen, K.V. Hansen, A. Hauch, T. Jacobsen, S.H. Jensen, T.L. Skafte, X. Sun, Reversible solid-oxide cells for clean and sustainable energy, Clean Energy 3 (2019) 175–201. https://doi.org/10.1093/ce/zkz023.

[54] M.S. Khan, X. Xu, R. Knibble, Z. Zhu, Air electrodes and related degradation mechanisms in solid oxide electrolysis and reversible solid oxide cells, Renew. Sust. Energy Rev. 143 (2021) 110918. https://doi.org/10.1016/j.rser.2021.110918.

[55] S. Hu, W. Li, H. Finklea, X. Liu, A review of electrophoretic deposition of metal oxides and its application in solid oxide fuel cells, Adv. Colloid Interface Sci. 276 (2020) 102102. https://doi.org/10.1016/j.cis.2020.102102.

[56] D. Salehzadeh, P. Marashi, Z. Sadeghian, Electrophoretic deposited $Ni(OH)_2$-YSZ and NiO-YSZ nanocomposite coatings, microstructural and electrochemical evaluation, Surf. Coat. Tech. 381 (2020) 125155. https://doi.org/10.1016/j.surfcoat.2019.125155.

[57] S. Obregón, G. Amor, A. Vázquez, Electrophoretic deposition of photocatalytic materials, Adv. Colloid Interface Sci. 269 (2019) 236-255. https://doi.org/10.1016/j.cis.2019.05.003.

[58] A.A. Daryakenari, B. Mosallanejad, E. Zare, M.A. Daryakenari, A. Montazeri, A. Apostoluk, J. Delaunay, Highly efficient electrocatalysts fabricated via electrophoretic deposition for alcohol oxidation, oxygen reduction, hydrogen evolution, and oxygen evolution reactions, Int. J. Hydrog. Energy 46 (2021) 7263–7283. https://doi.org/10.1016/j.ijhydene.2020.11.261.

[59] E. Pikalova, E. Kalinina, Place of electrophoretic deposition among thin-film methods adapted to the solid oxide fuel cell technology: A short review, Int. J. Energy Prod. and Mgm. 4 (2019) 1-27. https://doi.org/10.2495/EQ-V4-N1-1-27.

[60] A.J. Majewski, S.K. Singh, N.K. Labhasetwar, R. Steinberger-Wilckens, Nickel-molybdenum catalysts for combined solid oxide fuel cell internal steam and dry reforming, Chem. Eng. Sci. 232 (2021) 116341. https://doi.org/10.1016/j.ces.2020.116341.

* [61] Q. Bkour, F. Che, K.M. Lee, C. Zhou, N. Akter, J.A. Boscoboinik, K. Zhao, J.T. Gray, S.R. Saunders, M. Grant Norton, J.S McEwen, T. Kim, S. Ha, Enhancing the partial oxidation of gasoline with Mo-doped Ni catalysts for SOFC applications: An integrated experimental and DFT study, Appl. Catal. B 266 (2020) 118626. https://doi.org/10.1016/j.apcatb.2020.118626.

Bkour et al. introduced an internal reforming layer with the composition of Ni(11 wt.%)-Mo(3 wt.%)-YSZ at the Ni-YSZ anode of anode-supported single SOFC. This allowed for stable performance (with a low degradation rate) of an isooctane-fueled cell during the short-term stability test at the current density of 0.5 A/cm^2, while a similar cell without reforming layer failed after 12 h of operation. The DFT-based calculation suggested enhanced carbon tolerance of (Ni-Mo)/YSZ catalysts due to higher activation barriers for the C-H bond cleavage and C-C coupling as compared to Ni/YSZ system.

[62] X. Hou, K. Zhao, O.A. Marina, M. Grant Norton, S. Ha, NiMo-ceria-zirconia-based anode for solid oxide fuel cells operating on gasoline surrogate, Appl. Catal. B 242 (2019) 31-39. https://doi.org/10.1016/j.apcatb.2018.09.095.

* [63] M.J. Escudero, C.A. Maffiotte, J.L. Serrano, Long-term operation of a solid oxide fuel cell with MoNi-CeO_2 as anode directly fed by biogas containing simultaneously sulphur and siloxane, J. Power Sources 481 (2021) 229048. https://doi.org/10.1016/j.jpowsour.2020.229048.

Escudero et al. evaluated the long-term performance of a single cell with Ni-Mo-CeO_2 composite anode (Ni+Mo loading of 30 wt%, Ni:Mo = 5:1) fueled by simulated biogas contaminated with 10 ppm(v) of H_2S and 0.5 ppm(v) of D4 siloxane. The cell was tested at 750°C under a current density of 140 mA/cm^2 and showed a low degradation rate of only ~0.006 mW/h during 1737 h of operation. The impressively stable performance was attributed to improvements in catalytic activity for dry reforming of methane and carbon resistance of anode provided by Mo additions.

[64] S.A. Belyakov, S.N. Shkerin, D.G. Kellerman, M.S. Plekhanov, The effect of Mo concentration on the electrical properties of $CaV_{1-x}Mo_xO_{3-\delta}$ (x = 0.2 ÷ 0.6) anode materials for solid oxide fuel cells, Mater. Res. Bull. 129 (2020) 110904. https://doi.org/10.1016/j.materresbull.2020.110904.

[65] J. Macías, A.A. Yaremchenko, E. Rodríguez-Castellon, M. Starykevich, J.R. Frade, Compromising between phase stability and electrical performance: $SrVO_3$–$SrTiO_3$ solid solutions as solid oxide fuel cell anode components, ChemSusChem 12 (2019) 240-251. https://doi.org/10.1002/cssc.201801727.

[66] G. Carollo, A. Garbujo, F. Mauvy, A. Glisenti, Critical raw material-free catalysts and electrocatalysts: complementary strategies to activate economic, robust, and ecofriendly $SrTiO_3$, Energy Fuels 34 (2020) 11438-11448. https://doi.org/10.1021/acs.energyfuels.0c01678.

[67] B. Niu, F. Jin, J. Liu, Y. Zhang, P. Jiang, T. Feng, B. Xu, T. He, Highly carbon- and sulfur-tolerant $Sr_2TiMoO_{6-\delta}$ double perovskite anode for solid oxide fuel cells, Int. J. Hydrog. Energy 44 (2019) 20404-20415. https://doi.org/10.1016/j.ijhydene.2019.06.023.

[68] T. Feng, B. Niu, J. Liu, T. He, Sr- and Mo-deficiency $Sr_{1.95}TiMo_{1-x}O_{6-\delta}$ double perovskites as anodes for solid-oxide fuel cells using H_2S-containing syngas, Int. J. Hydrog. Energy 45 (2020) 23444-23454. https://doi.org/10.1016/j.ijhydene.2020.06.115.

[69] Y. Wan, Y. Xing, Y. Xie, N. Shi, J. Xu, C. Xia, Vanadium-doped strontium molybdate with exsolved Ni nanoparticles as anode material for solid oxide fuel cells, ACS Appl. Mater. Interfaces 11 (2019) 42271-42279. https://doi.org/10.1021/acsami.9b15584.

[70] V. Sadykov, A. Krasnov, Y. Fedorova, A. Lukashevich, Y. Bespalko, N. Eremeev, P. Skriabin, K. Valeev, O. Smorygo, Novel nanocomposite materials for oxygen and hydrogen separation membranes, Int. J. Hydrog. Energy 45 (2020) 13575–13585. https://doi.org/10.1016/j.ijhydene.2018.02.182.

[71] L. Bobrova, N. Eremeev, N. Vernikovskaya, V. Sadykov, O. Smorygo, Effect of asymmetric membrane structure on hydrogen transport resistance and performance of a catalytic membrane reactor for ethanol steam reforming, Membranes 11(5) (2021) 332. https://doi.org/10.3390/membranes11050332.

[72] I.V. Yentekakis, P. Panagiotopoulou, G. Artemakis, A review of recent efforts to promote dry reforming of methane (DRM) to syngas production via bimetallic catalyst formulations, Appl. Catal. B Environ. 296 (2021) 120210. https://doi.org/10.1016/j.apcatb.2021.120210.

[73] M.A.A. Aziz, H.D. Setiabudi, L.P. Teh, N.H.R. Annuar, A.A. Jalil, A review of heterogeneous catalysts for syngas production via dry reforming, J. Taiwan. Inst. Chem. Eng. 101 (2019) 139–158. https://doi.org/10.1016/j.jtice.2019.04.047.

[74] X. Gao, J. Ashok, S. Kawi, Smart designs of anti-coking and anti-sintering Ni-based catalysts for dry reforming of Methane: A recent review, Reactions 1 (2020) 162–194; https://doi.org/10.3390/reactions1020013.

[75] V.A. Sadykov, M.V. Arapova, E.A. Smal, S.N. Pavlova, L.N. Bobrova, N.F. Eremeev, N.V. Mezentseva, M.N. Simonov, Nanocomposite catalysts for transformation of biofuels into syngas and hydrogen: fundamentals of design and performance, application in structured reactors and catalytic membranes, in: J. Spivey, Y.-F. Han, D. Shekhawat (Eds.), Catalysis: Volume 31, Royal Society of Chemistry, 2019, pp. 216–241. https://doi.org/10.1039/9781788016971-00216.

[76] V. Sadykov, S. Pavlova, J. Fedorova, A. Bobin, V. Fedorova, M. Simonov, A. Ishchenko, T. Krieger, M. Melgunov, T. Glazneva, T. Larina, V. Kaichev, A.- C. Roger, Structured catalysts with mesoporous nanocomposite active components loaded on heat-conducting substrates for transformation of biogas/biofuels into syngas, Catal. Today (2020) https://doi.org/10.1016/j.cattod.2020.10.017.

[77] J.H.I. Wysocka, A. Rogala, Catalytic activity of nickel and ruthenium–nickel catalysts supported on SiO_2, ZrO_2, Al_2O_3, and $MgAl_2O_4$ in a dry reforming process, Catalysts 9 (2019) 13, https://doi.org/10.3390/catal9060540.

[78] A.C. Villagran-Olivares, M.F. Gomez, M.N. Barroso, M.C. Abello, Hydrogen production from ethanol: Synthesis of Ni catalysts assisted by chelating agents, Mol. Catal. 481 (2020) 110164. https://doi.org/10.1016/j.mcat.2018.08.006.

[79] A. Shahnazi, S. Firoozi, Improving the catalytic performance of $LaNiO_3$ perovskite by manganese substitution via ultrasonic spray pyrolysis for dry reforming of methane, Journal of CO_2 Utilization 45 (2021) 101455. https://doi.org/10.1016/j.jcou.2021.101455.

[80] E.A. Smal, M.N. Simonov, N.V. Mezentseva, T.A. Krieger, T.V. Larina, A.A. Saraev, T.S. Glazneva, A.V. Ishchenko, V.A. Rogov, N.F. Eremeev, E.M. Sadovskaya, V.A. Sadykov, Spinel-type $Mn_xCr_{3-x}O_4$-based catalysts for ethanol steam reforming, Appl. Catal. B Environ. 283 (2021) 119656, https://doi.org/10.1016/j.apcatb.2020.119656.

[81] S.M. Naurzkulova, M.V. Arapova, A.V. Ishchenko, T.A. Krieger, A.A. Saraev, V.V. Kaichev, V.A. Rogov, A.V. Krasnov, B.K. Massalimova, V.A. Sadykov, Ni–Ru-containing mixed oxide-based composites as precursors for ethanol steam reforming catalysts: Effect of the synthesis methods on the structural and catalytic properties. Open Chem. 19 (2021) 696–708. https://doi.org/10.1515/chem-2021-0062.

[82] M. Li, Z. Sun, Y.H. Hu, Catalysts for CO_2 reforming of CH_4: a review, J. Mater. Chem. A 9 (2021) 12495-12520. https://doi.org/10.1039/d1ta00440a.

[83] C. Wang, Y. Wang, M. Chen, D. Liang, Z. Yang, W. Cheng, Z. Tang, J. Wang, H. Zhang, Recent advances during CH_4 dry reforming for syngas production: A mini review, Int. J. Hydrogen Energy 46 (2021) 5852-5874. https://doi.org/10.1016/j.ijhydene.2020.10.240.

*[84] V.A. Sadykov, N.F. Eremeev, E.M. Sadovskaya, Y.A. Chesalov, S.N. Pavlova, V.A. Rogov, M.N. Simonov, A.S. Bobin, T.S. Glazneva, E.A. Smal, A.I. Lukashevich, A.V. Krasnov, V.I. Avdeev, A.-C. Roger, Detailed mechanism of ethanol transformation into syngas on catalysts based on mesoporous $MgAl_2O_4$ support loaded with Ru+Ni/(PrCeZrO or $MnCr_2O_4$) active components, Top. Catal. 63 (2020) 166–177. https://doi.org/10.1007/s11244-020-01222-1.

In situ FTIRS and ^{18}O SSITKA allowed to estimate rate constants of main reactions steps and to show that rate-limiting stage is incorporation of surface oxygen species into acetaldehyde or ethoxy species with C–C bond rupture yielding CO and CO_2 along with H_2 and H_2O.

*[85] N. Kumar, S. Kanitkar, Z. Wang, D. Haynes, D. Shekhawat, J.J. Spivey, Dry reforming of methane with isotopic gas mixture over Ni-based pyrochlore catalyst, Int. J. Hydrog. Energy 44 (2019) 4167-4176. https://doi.org/10.1016/j.ijhydene.2018.12.145

Transients with isotope –labeled reagents revealed that coke originates only from methane, while lattice oxygen of support is not involved in dry reforming reaction.

[86] A.V.P. Lino, C.B. Rodella, E.M. Assaf, J.M. Assaf, Methane tri-reforming for synthesis gas production using $Ni/CeZrO_2/MgAl_2O_4$ catalysts: Effect of Zr/Ce molar ratio, Int. J. Hydrogen Energy 45 (2020) 8418-8432. https://doi.org/10.1016/j.ijhydene.2020.01.002.

[87] S. Katheria, G. Deo, D. Kunzru, Rh-Ni/$MgAl_2O_4$ catalyst for steam reforming of methane: Effect of Rh doping, calcination temperature and its application on metal monoliths. Appl. Catal. A Gen. 570 (2019) 308–318 https://doi.org/10.1016/j.apcata.2018.11.021.